Original paper

Si-deficient foitite with [4]Al and [4]B from the 'Ługi-1' borehole, southwestern Poland

Adam PIECZKA[1*], Arkadiusz BUNIAK[2], Jarosław MAJKA[3], Hans HARRYSON[3]

[1] *Department of Mineralogy, Petrography and Geochemistry, AGH – University of Science and Technology, Mickiewicza 30, 30-059 Kraków, Poland; pieczka@agh.edu.pl*
[2] *Polish Oil and Gas Company (PGNiG S.A.), PGNiG Zielona Góra Branch, Westerplatte 15, 65-034 Zielona Góra, Poland*
[3] *Department of Earth Sciences, Uppsala University, Villavägen 16, SE-752 36 Uppsala, Sweden*
[*] *Corresponding author*

A tourmaline depleted in Si has been found in the cement of Upper Rotliegend aeolian sandstone overlaying Lower Rotliegend volcanic rock in the 'Ługi-1' prospecting borehole near Jarocin in the Fore-Sudetic Monocline, south-western Poland. Tourmaline, representing Mg-bearing foitite, crystallized around quartz grains in the form of radial aggregates of tiny crystals, reaching only 1–2 μm in diameter. Due to the very small size of the tourmaline crystals and the presence of significant contents of transitional metals in the crystal lattice, only direct determination of B_2O_3 in nm-sized spots enables evaluation of [4]Al and [4]B. Compositions of the tourmaline in successive analytical spots show that Si deficiency is supplemented both by [4]Al (0.00 to 0.48 Al apfu) as well as by [4]B (0.00 to 0.83 B apfu) at varying proportions. The origin of the mineral was related to diagenesis of evaporate sediments inducing reactions of quartz and clay minerals as primary components in the tourmaline-bearing sandstone with Ca saturated pore brines rich in Cl^- and $(BO_3)^{3-}$.

Keywords: Si-deficient tourmaline, tetrahedrally coordinated aluminum, tetrahedrally coordinated boron, Ługi borehole, Poland
Received: 25 September 2010; accepted: 22 November 2011; handling editor: M. Novák
The online version of this article (doi: 10.3190/jgeosci.105) contains supplementary electronic material.

1. Introduction

Tourmaline represents a supergroup of minerals with highly diversified compositions, whose chemical formulae can be written as $XY_3Z_6[T_6O_{18}][BO_3]_3V_3W$ (Hawthorne and Henry 1999; Henry et al. 2011), where *X* denotes Na^+, K^+, Ca^{2+}, □ [vacancy]; *Y* – Li^+, Mg^{2+}, Fe^{2+}, Mn^{2+}, Zn^{2+}, Al^{3+}, Cr^{3+}, V^{3+}, Fe^{3+}, Ti^{4+}; *Z* – Mg^{2+}, Al^{3+}, Cr^{3+}, V^{3+}, Fe^{3+}, Ti^{4+}; *T* – Si^{4+}, Al^{3+}, B^{3+}; *B* – B^{3+}, □; *V* – OH^-, O^{2-} and *W* – OH^-, F^-, O^{2-}. Recently, the possibility of Al and B substitution for Si in the tetrahedral *T* site has been one of the most interesting structural problems studied. For many years, it has been accepted that Al can supplement a small deficiency of Si (e.g. Povondra 1981). Structure refinements of some crystals representing various members of the tourmaline group corroborate this substitution (Grice and Ercit 1993; MacDonald and Hawthorne 1995; Bloodaxe et al. 1999; Prowatke et al. 2003; Ertl et al. 2003; Cempírek et al. 2006).

Boron is one of the main components of tourmaline; however, difficulties in chemical determination of this element result in the common assumption that its content in the tourmaline formula unit is equal to the 3.0 atoms required to fill the *B* site completely. Nevertheless, an excess of boron over 3.0 atoms per formula unit (*apfu*) has been observed in compositions of some tourmaline crystals for which B_2O_3 was determined directly (e.g. Barton 1969; Dyar et al. 1994, 1998). Such elevated B content indicates that the *B* site is completely filled by the element, and the surplus has to enter another cationic lattice position. A partial replacement of Si by B was proposed by Barton (1969) and, later, by Serdyuchenko (1980). Only structural investigations of olenite from Stoffhütte, Austria (Ertl et al. 1997; Hughes et al. 2000) with a significant excess of boron (close to 1.0 apfu) and the lowest measured <*T*–O> mean bond length (1.609–1.610 Å), unequivocally proved that the Si deficiency in tourmaline can be supplemented not only by Al, but also by B. Wodara and Schreyer (1997, 1998, 2001), Schreyer et al. (2000) and Marler et al. (2002) synthesized an *X*-site vacant, Al-bearing tourmaline and olenite with significant contents of [4]B reaching *c.* 1.4 and 2.2–2.3 apfu, respectively. Since then, the presence of [4]B has been noted in many natural crystals of tourmaline rich in Al. The crystals commonly represent olenite (Ertl et al. 1997; Hughes et al. 2000, 2004; Schreyer et al. 2002), elbaite (Tagg et al. 1999; Hughes et al. 2001), members of the liddicoatite–elbaite series (Ertl et al. 2006), rossmanite (Ertl et al. 2005), an Al-rich tourmaline (Ertl et al. 2008) and, only exceptionally, other tourmaline varieties such as schorl (Ertl and Hughes 2002) or dravite (Marschall et al. 2004).

In this paper, we describe extremely fine-crystalline, Si-depleted, Fe-bearing tourmaline found in Permian evaporate

sediments in an oil-prospecting borehole in south-western Poland. To date, only Hancock (1978) has noted tourmaline in the Rotliegend sandstone of northwestern Germany.

2. Geological setting

The European Rotliegend Basin with numerous natural gas deposits extends from the eastern England coast, through Holland and northern Germany to western and central Poland. This area is very attractive for the gas prospection due to geological and thermodynamic conditions favoring the generation and accumulation of large amounts of gas hydrocarbons, genetically related to the Carboniferous host rocks. In Poland, exploration of natural gas in sandstones of the Upper Rotliegend has been underway since the mid-1960's. Recently, in one of the prospecting boreholes, 'Ługi-1', near Śrem and Jarocin, south-western Poland, Si-depleted tourmaline was found in the cement of the aeolian sandstone (Buniak 2009).

The 'Ługi-1' borehole is situated in the northern part of the Fore-Sudetic Monocline, within the border region of the Upper Rotliegend Basin next to the margin of the Wolsztyn High (Fig. 1). Eruptive rocks of the Wielkopolska volcanic formation form the foundation of the sedimentary series of Upper Rotliegend (Pokorski 1981). In the nearby boreholes of Dolsk-1, Wyrzeka-1 and Książ Wlkp.-3, rhyolite, dacite and andesite have been found (Jackowicz 1994). The overlaying Upper Rotliegend sediments are represented by sandstone corresponding to the Noteć (Pokorski 1981) and the Siekierki (Karnkowski 1987) formations or the sedimentary sequence 8b (Kiersnowski 1997). The sandstone, formed mostly in an arid environment, relates to the final sedimentation stage in the East Erg next to the Wolsztyn High. The transgression of the Zechstein Sea stopped the deposition of sand-drift

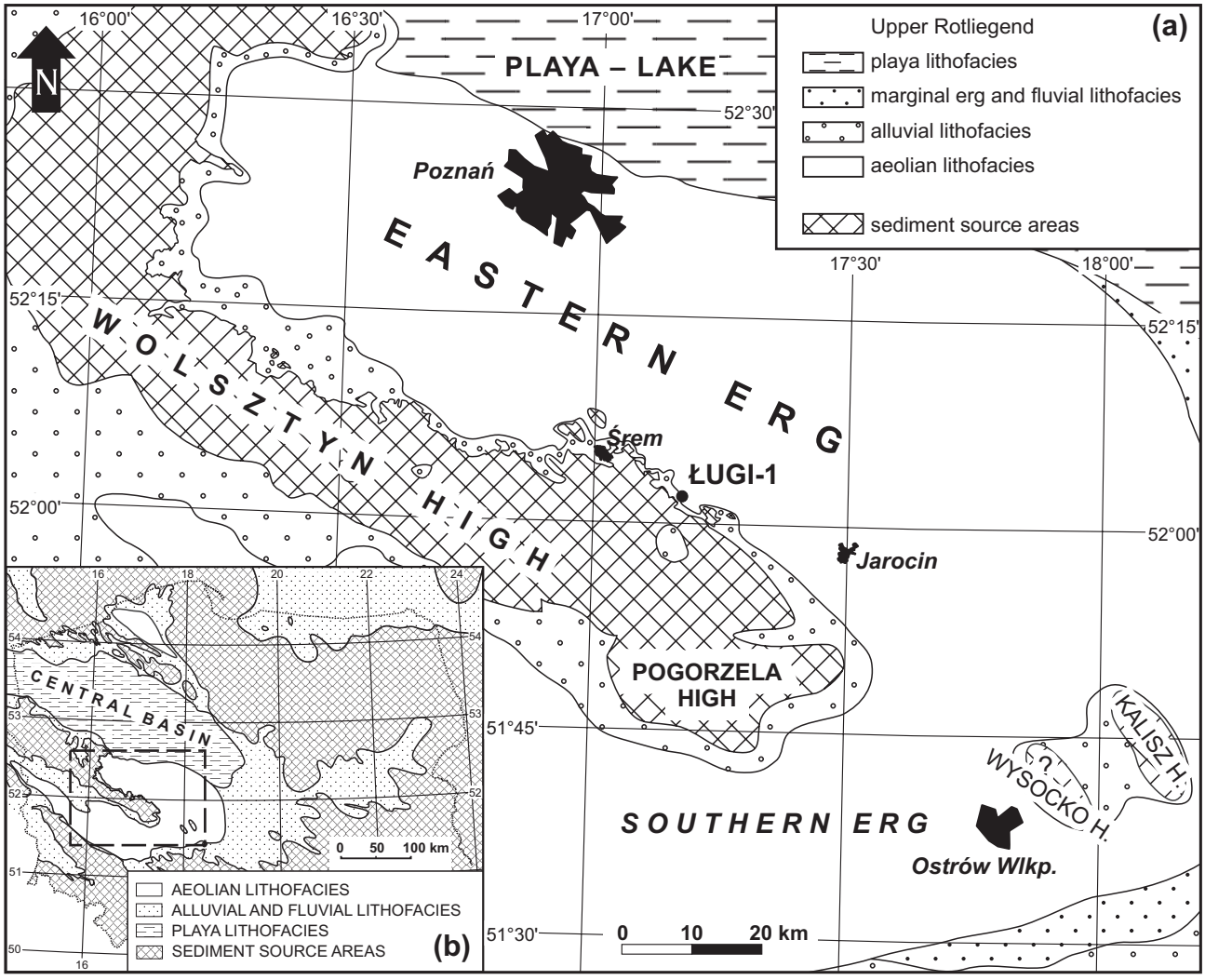

Fig. 1a A map of the Polish Upper Rotliegend Basin with localization of the 'Ługi-1' borehole. **b –** Overall geometry of the Polish Upper Rotliegend Basin (after Pokorski 1988, modified by Kiersnowski 1997).

formations, and the Rotliegend sediments are covered by evaporate rocks of the Werra cyclothem.

In the 'Ługi-1' prospecting borehole, the Upper Rotliegend sediments, with a thickness of only *c.* 9.3 m (2652.7–2662.0 m depth range), form a higher part of the Lower Permian formations. Below, up to 2700.0 m, occur Lower Rotliegend volcanics. The sedimentary profile is initiated by reddish brown, fine-grained sandstones and conglomerates deposited in an alluvial environment (0.2 m), resting immediately on volcanics. In the hanging wall occurs horizontally and diagonally bedded, fine- to medium-grained sandstone (7.7 m) grey in colour, which is related to an arid environment. The diagonally bedded sandstone represents the sand-drift core facies, whereas the horizontally and low-angle-diagonally bedded sandstone corresponds to the sand-drift base and inter-sand-drift facies. In the apical part of the complex, there is grey, horizontally bedded, fine-grained sandstone (1.4 m) formed in a shallow marine basin.

The tourmaline-bearing sandstone is a fine-grained and porous variety with a mean grain diameter of 0.18–0.23 mm and moderately to very well sorted out grains, corresponding to quartz and sublithic arenites. The grain facies of the sandstone is composed of pieces of quartz and volcanic clasts, whereas tourmaline, calcite, dolomite, ankerite, anhydrite, halite, quartz and occasionally clay minerals form the cement. An unidentified Ca-chloride (antarcticite, $CaCl_2 \cdot 6H_2O$, or sinjarite, $CaCl_2 \cdot 2H_2O$) in the form of strongly elongated acicular microcrysts was observed in the pores. Tourmaline, whose content can be estimated at up to 0.X vol. % of the bulk rock, is a rather common component in the cement of the sandstone. The tourmaline crystallized around quartz grains (also occasionally around carbonates) in radial aggregates of tiny crystals, reaching 10 μm in length and only 1–2 μm in diameter (Fig. 2). In the aggregates, tourmaline forms perfect trigonal prisms and parallel intergrowths of two or three crystals.

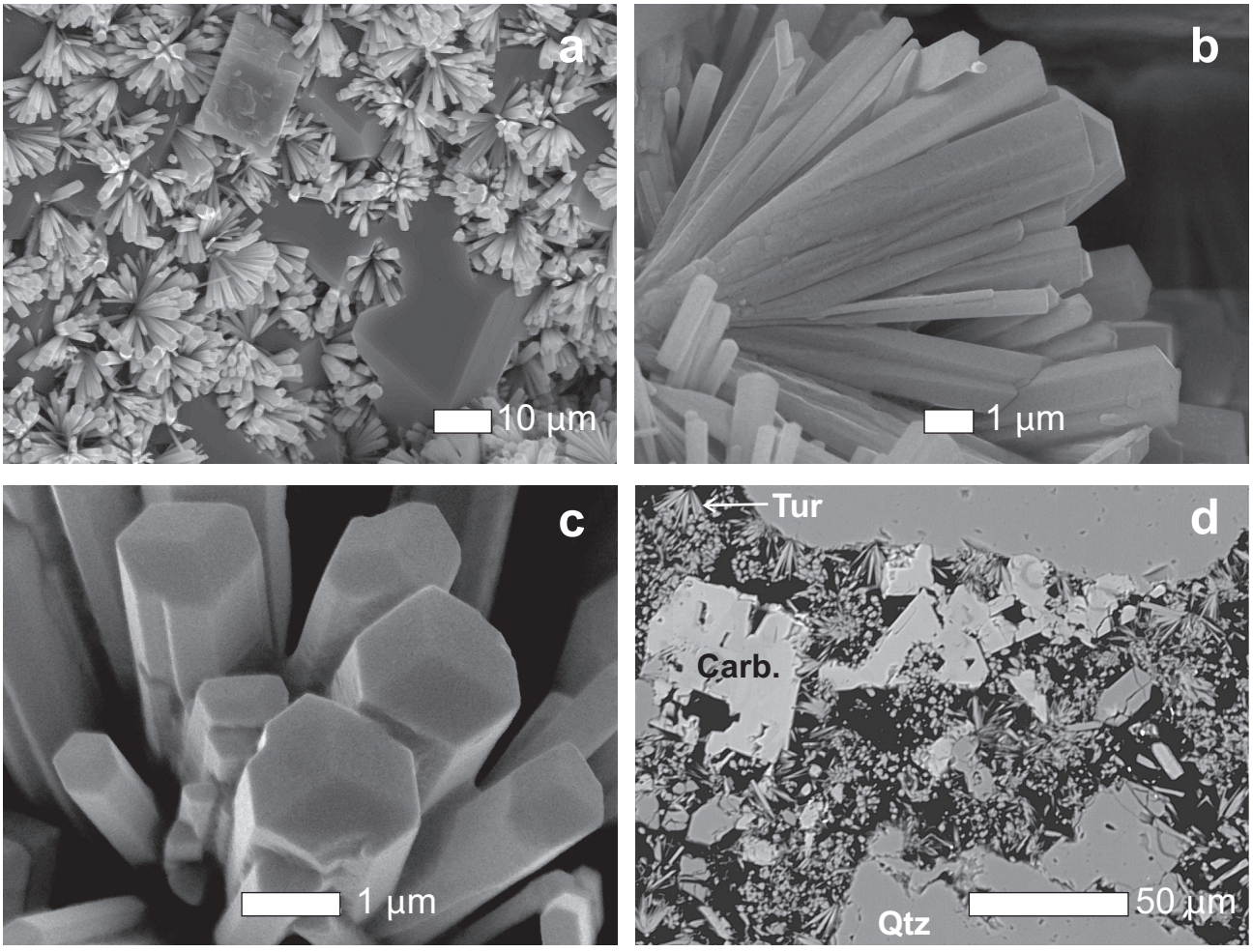

Fig. 2 Secondary electron microscope (SEM) images of the 'Ługi-1' tourmaline **(a–c)** and a BSE image of the 'Ługi' sandstone with numerous tourmaline crystals overgrowing quartz grains and carbonate rhombohedra **(d)**.

3. Methods

Samples for electron microprobe determinations were prepared from the tourmaline-bearing sandstone in a form of 1-inch epoxy discs, polished and coated with carbon. Initial electron microprobe analyses of the tourmaline have been carried out at the Inter-Institute Analytical Complex for Minerals and Synthetic Substances of Warsaw University with a CAMECA SX 100 electron microprobe, operating in the wave-length-dispersive (WDS) mode under the following conditions: accelerating voltage of 15 kV, beam current of 20 nA, focused beam with a diameter of ~1 μm, peak count-time 20 s and background time 10 s. The contents of all measured components were calculated in relation to the respective K_α analytical lines of the following standards: F – phlogopite (TAP), Na – albite (TAP), Mg and Si – diopside (TAP), Al – corundum (TAP), Cl – tugtupite (PET), K – orthoclase (PET), Ca – wollastonite (PET), Ti – rutile (PET), Mn – rhodonite (LIF), Fe – hematite (LIF), Zn – sphalerite (LIF), Cr – Cr_2O_3 (PET) and V – V_2O_5 (PET). The raw analyses were corrected with the PAP procedure (Pouchou and Pichoir 1985) applied by the Cameca.

The composition of tourmaline crystals investigated has been normalized in two different ways: (1) in relation to $Y + Z + T = 15$ apfu, stoichiometric B = 3 apfu and OH + F + Cl = 4 pfu, assuming the presence of only $^{[4]}$Al supplementing Si deficiency at the *T* site; (2) in relation to Si + B = 9 apfu and OH + F + Cl = 4 pfu, assuming the presence of only $^{[4]}$B supplementing Si deficiency at the *T* site. In both cases, Fe^{3+} was calculated from the charge balance in the tourmaline formula with 31 (O,OH,F,Cl). The depletion of Si in the tourmaline is clearly visible in its energy-dispersive (EDS) spectra, where the intensity of the AlK_α analytical line, for tourmaline commonly comparable with the SiK_α line, distinctly predominates in spite of moderate Al contents in that tourmaline. In such cases, the Si deficiency in the *T* site must be supplemented by $^{[4]}$Al, $^{[4]}$B or by both cations simultaneously. The recognition of a proper substitution at the *T* site is rather easy based on structural studies. The substitution of Al^{3+} for Si^{4+} is connected with an increase in the observed <*T*–O> mean bond length from *c.* 1.620 Å, a mean value typical of the Si–O bond, to a higher value due to a much longer $^{[4]}$Al–O bond (~1.74–1.75 Å). In contrast, the substitution of B^{3+} for Si^{4+} results in a decrease in the observed <*T*–O> mean bond length below 1.620 Å due to a much shorter $^{[4]}$B–O bond length close to only 1.47 Å (Hawthorne 1996). Identification of the replacements is less obvious in the case of the simultaneous presence of $^{[4]}$B and $^{[4]}$Al, because the opposite effects of these ions on <*T*–O> mean bond length can balance each other, and the observed <*T*–O> value can also be close to 1.620 Å, apparently reflecting the presence of 6.0 Si apfu at the *T* site. Unfortunately, the very small dimensions of the tourmaline crystals rule out the X-ray investigation using the single crystal method. Purification of the tourmaline is impossible in heavy liquids and in any acid mixture. Consequently, a structural study with the use of the Rietveld method could not be done. Magic-angle-spinning nuclear magnetic resonance (MAS-NMR) spectroscopy, commonly applied for detecting $^{[4]}$B and $^{[4]}$Al in tourmaline (Tagg et al. 1999; Marler and Ertl 2002; Marler et al. 2002; Lussier et al. 2009), also cannot be applied due to the very high presence of paramagnetic Fe ions. Lussier et al. (2009) did show that a high content of paramagnetic ions results in a dramatic decrease of intensity, and the recorded spectra are illegible. Ertl et al. (2008), studying Al-tourmaline with $^{[4]}$B, corrected a co-variation between the cell volume of $^{[4]}$B-bearing tourmalines and $^{[4]}$B contents in their structures, which was previously proposed by Wodara and Schreyer (2001) and Marler et al. (2002), allowing for estimation of the $^{[4]}$B content from X-ray powder diffraction data. However, this relationship is valid only for Al-rich tourmalines, especially olenite, where the *T* site is occupied only by Si and B, without significant $^{[4]}$Al, and contents of transitional metals are low. For Fe-bearing tourmalines, the relationship is more complex and prevents such estimation. Thus, none of the techniques mentioned above commonly used in the detection of $^{[4]}$Al and $^{[4]}$B in tourmaline can be used to recognize what kind of Si replacement exists in the 'Ługi' material. Therefore, we realized that direct determination of B_2O_3 content is indispensable for further discussion and only possible issue in such impasse situation. Due to the extremely low dimensions of the tourmaline crystals, we accepted only a microprobe determination with the use an apparatus that enables analyses in nm-scale spots.

Attempts at direct determination of B content in the tourmaline carried out at the above mentioned laboratory with CAMECA SX 100 microprobe (6 kV, 150 nA, PC2 crystal, SRM93a standard, K_α analytical line) gave satisfactory results only in a few cases (11.60–13.33 wt. % B_2O_3). These suggested the real possibility of a $^{[4]}$B presence in the material studied. However, in many cases, the determined B content was too low to be accepted, even for tourmaline with stoichiometric B = 3.0 apfu. Such negative results were probably due to the extremely small size of tourmaline crystals with transversal diameters of only ~1–2 μm; i.e. comparable with a size of analytical spot even with the use of completely focused beam. The porosity of the host rock could have played a role as well.

As a consequence, the final direct determinations of B_2O_3 contents were performed at the Centre for Experimental Mineralogy, Petrology and Geochemistry of the Department of Earth Sciences at Uppsala University, Sweden, using a JEOL JXA 8530F Field Emission Hyperprobe. The apparatus was operating under the following conditions: accelerating voltage of 15 kV, beam current of

10 nA, focused beam with a diameter of 0.X μm, counting time of 10 s on peak and 5 s on both (+) and (–) backgrounds. The contents of all measured components were standardized in relation to respective K_α analytical lines of the following standards: B – pure B (LDE2), F – LiF (TAP), Na – albite (TAP), Si, Ca – wollastonite (TAP), Mg – MgO (TAP), Al – Al_2O_3 (TAP), K – orthoclase (PETJ), Ti – pyrophanite (PETJ), Mn – pyrophanite (LIFH), Cl – vanadinite (PETH), Fe – Fe_2O_3 (LIFH), Zn – ZnS (LIFH). The data were reduced using the PAP procedure. The obtained tourmaline compositions have been normalized to $Y + Z + B + T = 18$ apfu with H_2O and Fe^{3+}/Fe_{total} ratio calculated stoichiometrically, assuming $(OH,F,Cl)^- = 4$ ions pfu and an electroneutral formula with 31 (O,OH,F,Cl).

4. Results and discussion

The complete set of the spot EMP analyses of the 'Ługi' tourmaline performed at Warsaw University is presented in the Electronic supplementary data, statistics for which is given in Tab. 1. The tourmaline shows a low SiO_2 content, only 32.18 wt. % as a mean value,

Tab. 1 Statistical distribution of of Si-deficient foitite compositions from the 'Ługi' borehole

	Si-deficient foitite (*n = 25*)				'normal' foitite (*n = 3*)			
	$^{IV}Al \rightarrow Si$		$^{IV}B \rightarrow Si$		$^{IV}Al \rightarrow Si$		$^{IV}B \rightarrow Si$	
	range	mean	range	mean	range	mean	range	mean
	wt. %				**wt. %**			
SiO_2	31.26 – 33.77	32.18	31.26 – 33.77	32.18	34.90 – 34.96	34.93	34.90 – 34.96	34.93
B_2O_3	9.78 – 10.36	9.94	11.49 – 13.01	12.40	10.14 – 10.39	10.27	10.20 – 11.45	10.86
Al_2O_3	33.06 – 35.99	34.24	33.06 – 35.99	34.24	33.02 – 34.34	33.75	33.02 – 34.34	33.75
Fe_2O_3	0.45 – 2.36	1.42	1.43 – 3.94	2.68	0.00 – 0.36	0.12	0.00 – 0.90	0.00
MgO	2.56 – 3.71	2.96	2.56 – 3.71	2.96	3.15 – 3.54	3.30	3.15 – 3.54	3.30
CaO	0.23 – 0.86	0.52	0.23 – 0.86	0.52	0.35 – 0.61	0.49	0.35 – 0.61	0.49
FeO	8.14 – 10.13	9.94	6.78 – 9.34	8.14	10.31 – 11.05	10.65	10.31 – 10.58	10.75
Na_2O	0.67 – 1.13	0.89	0.67 – 1.13	0.89	0.97 – 1.22	1.08	0.97 – 1.22	1.08
H_2O	3.29 – 3.54	3.37	3.44 – 3.67	3.52	3.27 – 3.53	3.36	3.30 – 3.59	3.44
Cl_2	0.00 – 0.52	0.21	0.00 – 0.52	0.21	0.23 – 0.44	0.35	0.23 – 0.44	0.35
$-O=Cl_2$	–0.12 – 0.00	–0.05	–0.12 – 0.00	–0.05	–0.10 – –0.05	–0.08	–0.10 – –0.05	–0.08
Total	93.59 – 98.78	94.95	96.38 –101.33	97.68	96.86 – 99.63	98.21	96.93 – 100.80	98.88
	apfu				**apfu**			
Na^+	0.220 – 0.377	0.303	0.212 – 0.368	0.291	0.317 – 0.396	0.353	0.314 – 0.389	0.350
Ca^{2+}	0.043 – 0.163	0.098	0.042 – 0.157	0.094	0.064 – 0.110	0.089	0.064 – 0.109	0.088
□	0.468 – 0.732	0.599	0.487 – 0.739	0.615	0.512 – 0.590	0.558	0.577 – 0.590	0.562
ΣX	1.000	1.000	1.000	1.000	1.000	1.000	1.000	1.000
$^{Y}Mg^{2+}$	0.648 – 0.978	0.772	0.625 – 0.944	0.741	0.794 – 0.882	0.832	0.785 – 0.867	0.824
$^{Y}Fe^{2+}$	1.200 – 1.501	1.356	0.952 – 1.320	1.143	1.458 – 1.545	1.507	1.443 – 1.515	1.470
$^{Y}Al^{3+}$	0.568 – 0.788	0.685	0.813 – 1.157	0.778	0.528 – 0.748	0.646	0.569 – 0.772	0.669
$^{Y}Fe^{3+}$	0.060 – 0.314	0.187	0.182 – 0.496	0.338	0.000 – 0.045	0.015	0.000 – 0.111	0.037
ΣY	3.000	3.000	3.000	3.000	3.000	3.000	3.000	3.000
$^{Z}Al^{3+}$	6.000	6.000	6.000	6.000	6.000	6.000	6.000	6.000
B^{3+}	6.000	6.000	6.000	6.000	6.000	6.000	6.000	6.000
$^{T}Si^{4+}$	5.518 – 5.794	5.628	5.238 – 5.664	5.405	5.847 – 5.990	5.913	5.749 – 5.984	5.858
$^{T}B^{3+}$	0.000	0.000	0.336 – 0.762	0.595	0.000	0.000	0.016 – 0.251	0.142
$^{T}Al^{3+}$	0.206 – 0.482	0.372	0.000	0.000	0.010 – 0.153	0.087	0.000	0.000
ΣT	6.000	6.000	6.000	6.000	6.000	6.000	6.000	6.000
O^{2-}	27.000	27.000	27.000	27.000	27.000	27.000	27.000	27.000
OH^-	3.847 – 4.000	3.937	3.853 – 4.000	3.940	3.684 – 3.934	3.793	3.730 – 3.935	3.811
Cl^-	0.000 – 0.153	0.063	0.000 – 0.147	0.060	0.066 – 0.127	0.101	0.065 – 0.126	0.100

B_2O_3 contents calculated from stoichiometry
Contents of K, Ti, Mn, V, Cr, Zn and F are below the respective detection limits; *n* – number of analyses.

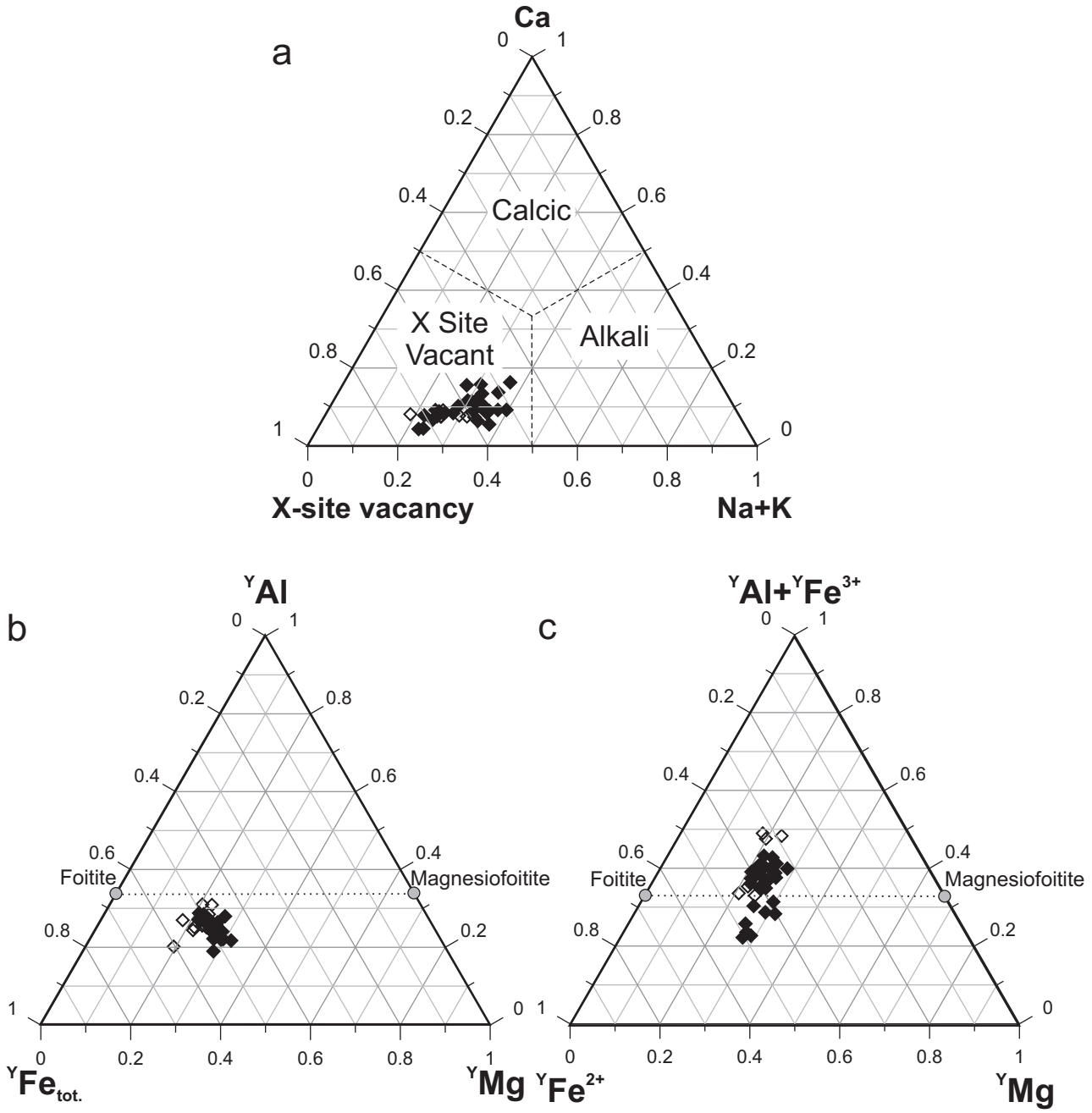

Fig. 3 Compositional relationships in the 'Ługi' tourmaline: **a –** the X site occupants; **b–c** the Y site occupants. Symbols: black diamonds – compositions with B_2O_3 content calculated from stoichiometry; white diamonds – compositions with direct EMP determination of B_2O_3 contents.

and the Al_2O_3 content, 34.24 wt. %, rather typical of many tourmaline crystals representing schorl, dravite, buergerite, foitite or magnesiofoitite varieties. All spot analyses of the tourmaline indicate a high deficiency in alkali cations, resulting in predominance of vacancy at the *X* site and, on the other hand, predominance of Fe over Mg and Al at the *Y* site (Fig. 3). This suggests unequivocally that the tourmaline has a composition transitional between foitite and magnesiofoitite end-members and can be classified as Mg-bearing foitite, using a new nomenclature of the tourmaline supergroup (Henry et al. 2011).

Table 1 presents statistics of two excessive cases of tourmaline compositions with the B_2O_3 contents calculated from stoichiometry assuming: (1) Si-deficiency supplemented solely by $^{[4]}$Al, (2) Si-deficiency compensated by $^{[4]}$B. If the presence of only $^{[4]}$Al substituted for Si is assumed, totals of all EMP analyses of Si-deficient tourmaline range from *c.* 93.6 to 98.8 wt. % with a mean value of 95.0 wt. %. On the other hand, analyses in areas

Tab. 2 Representative compositions of Si-deficient foitite from the 'Ługi' borehole, with direct EMP determinations of B_2O_3 contents

	6	12	15	26	27	28	31	47	50	57
					wt. %					
SiO_2	31.78	32.78	33.35	32.73	33.56	34.22	33.67	33.52	32.32	30.47
B_2O_3	13.64	10.28	10.39	10.70	12.29	11.98	11.05	11.21	13.49	12.33
Al_2O_3	35.97	36.63	37.05	35.99	34.98	35.17	36.30	35.81	35.68	33.71
Fe_2O_3	4.41	2.49	2.00	3.27	2.73	2.07	2.61	0.75	5.58	6.56
MgO	2.86	2.82	2.87	2.66	2.90	3.06	2.70	2.52	2.31	2.36
CaO	0.35	0.28	0.29	0.36	0.31	0.29	0.38	0.33	0.33	0.35
FeO	6.34	8.44	8.73	8.67	8.84	9.33	9.33	9.81	7.26	6.88
Na_2O	0.83	0.83	0.84	0.80	0.98	1.04	0.84	0.85	0.64	0.80
H_2O	3.65	3.53	3.54	3.47	3.65	3.67	3.54	3.58	3.70	3.38
F_2	0.00	0.00	0.00	0.21	0.00	0.00	0.18	0.00	0.00	0.26
Cl_2	0.12	0.12	0.22	0.05	0.04	0.00	0.05	0.02	0.02	0.05
$–O=F_2$	0.00	0.00	0.00	–0.09	0.00	0.00	–0.08	0.00	0.00	–0.11
$–O=Cl_2$	–0.03	–0.03	–0.05	–0.01	–0.01	0.00	–0.01	0.01	–0.01	–0.01
	99.91	98.18	99.24	98.81	100.27	100.84	100.57	98.39	101.34	97.03
					apfu					
$^{X}Na^{+}$	0.262	0.272	0.271	0.261	0.311	0.330	0.268	0.275	0.201	0.263
$^{X}Ca^{2+}$	0.061	0.051	0.051	0.065	0.054	0.051	0.067	0.059	0.057	0.064
^{X}vac.	0.677	0.676	0.678	0.674	0.635	0.619	0.664	0.666	0.742	0.673
ΣX	1.000	1.000	1.000	1.000	1.000	1.000	1.000	1.000	1.000	1.000
$^{Y}Mg^{2+}$	0.693	0.708	0.714	0.665	0.709	0.745	0.663	0.628	0.558	0.599
$^{Y}Fe^{2+}$	0.863	1.189	1.216	1.216	1.213	1.274	1.285	1.372	0.981	0.980
$^{Y}Al^{3+}$	0.900	0.797	0.831	0.706	0.741	0.727	0.729	0.905	0.784	0.580
$^{Y}Fe^{3+}$	0.540	0.316	0.251	0.413	0.337	0.255	0.324	0.095	0.678	0.841
ΣY	2.997	3.011	3.012	3.000	3.000	3.000	3.000	3.000	3.000	3.000
$^{Z}Al^{3+}$	6.000	6.000	6.000	6.000	6.000	6.000	6.000	6.000	6.000	6.000
B^{3+}	3.000	2.989	2.988	3.000	3.000	3.000	3.000	3.000	3.000	3.000
$^{T}Si^{4+}$	5.173	5.522	5.556	5.491	5.503	5.586	5.544	5.608	5.223	5.189
$^{T}B^{3+}$	0.831	0.000	0.000	0.099	0.478	0.375	0.141	0.237	0.764	0.624
$^{T}Al^{3+}$	0.000	0.478	0.444	0.410	0.019	0.039	0.315	0.156	0.013	0.186
ΣT	6.003	6.000	6.000	6.000	6.000	6.000	6.000	6.000	6.000	6.000
$O^{2–}$	27.000	27.000	27.000	27.000	27.000	27.000	27.000	27.000	27.000	27.000
$OH^{–}$	3.967	3.966	3.938	3.878	3.988	4.000	3.893	3.993	3.994	3.845
$F^{–}$	0.000	0.000	0.000	0.109	0.000	0.000	0.094	0.000	0.000	0.140
$Cl^{–}$	0.033	0.034	0.062	0.013	0.012	0.000	0.013	0.007	0.006	0.015

corresponding to tourmaline with a low Si deficiency ('normal' foitite) sum up to 96.9 to 99.6 wt. %, with a mean of 98.2 wt. %. The same analyses recalculated with an excess of B supplementing the Si deficiency reach totals ranging from 96.4 to 101.3 wt. % (mean 97.7 wt. %), and 96.9 to 100.8 wt. % (mean 98.9 wt. %), respectively. The low analytical totals for both types of substitution for Si at the *T* site can be easily explained by the shortcomings of microprobe analyses due to the very small size of the tourmaline crystals, infiltration of epoxy into voids within the cement of the sandstone and analysis of the target material diluted by epoxy. However, the mean totals for Si-deficient and 'normal' foitite are closer to each other in case when $^{[4]}$B is assumed. This suggests that B could indeed substitute for Si in the tourmaline.

Electron microprobe analyses with direct determination of B_2O_3 (Tab. 2) corroborate its elevated contents of almost 10.3 to above 13.6 wt. % in many tourmaline crystals. Chemical formulae calculated for successive spots, based on 31 (O,OH,F,Cl), show that Si deficiency in the 'Ługi' tourmaline is supplemented by $^{[4]}$Al with $^{[4]}$B at varying proportions (0.00–0.48 Al and 0.00–0.83 B apfu). The occurrence of the $^{[4]}$Al and $^{[4]}$B substitution for Si corresponds to the predicted conditions of the tourmaline formation (low temperature and low pressure). Higher temperatures and/or pressures would favour the substitution of Al for Si (Ertl et al. 2008).

However, the 'Ługi' tourmaline displays some apparent discrepancies in relation to the 'rules' noted in literature, referring to the presence of $^{[4]}$B or $^{[4]}$Al in the mineral. Hawthorne (1996) showed that trivalent substituents at the *T* site must be locally associated with Al at the adjacent *Y* and *Z* sites, and the *X* site should be occupied by Ca. Hughes et al. (2000) pointed out that Na can also occupy the *X* site adjacent to a tetrahedron containing $^{[4]}$B. In fact, $^{[4]}$B is commonly found in tourmalines with $^{[6]}$Al > 7.0 apfu, but there are exceptions. For instance, 0.25 $^{[4]}$B apfu was discovered in schorl with lower content of 6.78 $^{[6]}$Al apfu (Ertl and Hughes 2002). In Mg-rich tourmalines, Si deficiency should be compensated by $^{[4]}$Al (e.g. MacDonald and Hawthorne 1995; Bloodaxe et al. 1999). Ertl and Hughes (2002) suggested that only tourmalines with low Mg,

even schorls, and with a high olenite component can contain significant $^{[4]}$B. This was corroborated by MAS NMR investigations of magnesiofoitite (Lussier et al. 2009), which did not show $^{[4]}$B. However, Marschall et al. (2004), based on structural investigations of a metamorphic dravite from Syros, Greece, concluded that 'substantial contents of Mg at the *Y* site or at the *Z* site do not exclude the possibility of the occurrence of $^{[4]}$B'. Next, the *X* ions coordinate, among others, the *O(4)* and *O(5)* bridge oxygens between the adjacent tetrahedra; thus, the presence of trivalent substituents at the *T* site can only gain a bond-valence contribution from adjacent *T* and *X* cations. Ertl et al. (2008) concluded that 'the possible charge-balance mechanisms require the *X* site to be occupied and can only have a small portion of vacancies, and the *V* and *W* sites must be occupied by higher total contents of OH up to 4 pfu'. However, this is also not a rule, because $^{[4]}$B was also observed in rossmanite with the *X* site dominated by vacancy (Ertl et al. 2005). Hughes et al. (2004) commented the composition of the richest in $^{[4]}$B olenite from Stoffhütte with a high *X* site vacancy that 'despite the charge-balancing valence provided by the *X* site occupant, it is not necessary to have an adjacent *X* site occupant for the charge balance in $^{[4]}$B-substituted tourmaline'. In the Si-deficient, Mg-bearing 'Ługi' foitite, the increase in $^{[4]}$B and $^{[4]}$Al relates to an increase in $^{[Y]}Al^{3+} + {}^{[Y]}Fe^{3+}$ (Fig. 3b–c). Thus, the substitution $^{[T]}Si + {}^{[Y]}Me^{2+} = {}^{[T]}(Al^{3+}, B^{3+}) + {}^{[Y]}(Al^{3+}, Fe^{3+})$, analogous with that proposed by Kalt et al. (2001) for tourmalines of the schorl–dravite to olenite series, including $^{[4]}$B, satisfies the bond-valence requirements, referring to the presence of trivalent substituents at the *T* site of the tourmaline structure.

Another important question is the origin of the 'Ługi' tourmaline. The tourmaline cannot be a result of the action of B- and Cl-rich fluids released by the underlying volcanic rock, because the Lower Rotliegend volcanics are older than the tourmaline-bearing Upper Rotliegend sandstone deposited on them, which contains volcanic clasts at its base. In addition, the volcanics do not show any signs of tourmalization, not even next to the tourmaline-bearing sandstone. On the other hand, it is also very unlikely that B- and Cl-rich fluids were released from the overlying evaporate rocks of the Werra cyclothem, because tourmaline has only been found in a relatively thin bed occurring immediately below the evaporate sequence. Additionally, this tourmaline composition, corresponding to Mg-bearing foitite with vacancy predominating in the *X* site, does not fit to an expected, strongly Na-enriched composition of such potential fluids derived from evaporates.

Thus the source of boron needed for tourmaline crystallization could be related only to sand-drift sands and sediments of desert areas periodically flooded by water, or of ephemeral salt lakes, lagoons or a shallow epicontinental sea, deposited in the arid climate of Upper Rotliegend. Under such conditions, Cl^- and $(BO_3)^{3-}$ ions could have migrated into the groundwater system, and Cl^- and $(BO_3)^{3-}$-rich brines, also containing other common ions like Na^+, Ca^{2+}, Mg^{2+} and Fe^{2+}, could have entered into pore waters present in the sands. The brines could have further been modified by infiltration, compaction or dehydration of clay minerals and saturated in Ca by interaction with the overlaying Border Limestone and Lower Anhydrite units of the Werra cyclothem. Diagenetic processes could have induced reactions of the brines with quartz and clay minerals as primary components in the sands resulting in, among others, crystallization of Na-deficient tourmaline enriched in $^{[4]}$Al and $^{[4]}$B. The observed presence of an unrecognized $CaCl_2$ phase (antarcticite or sinjarite) crystallized in small voids into cement of the sandstone among tourmaline crystals proves Ca saturation in the brines. Both minerals, strongly hygroscopic and easily dissolved, were never found in typical evaporate rocks, but they precipitate from highly saline Ca-saturated brines under very arid conditions (Dunning and Cooper 1969; Aljubouri and Aldabbagh 1980). In the tourmaline-bearing Permian sandstones of the 'Ługi' borehole, they can represent a phase that crystallized contemporarily from the pore brines.

5. Conclusions

1. Tourmaline found in the cement of Upper Rotliegend sandstone in the 'Ługi' borehole represents Si-depleted, Mg-bearing foitite. Direct EMP determination of B_2O_3 showed varying and, very often, elevated content of the component, reaching 13.64 wt. %. The calculated formula unit indicates that Si deficiency is supplemented by Al (0.00–0.48 $^{[4]}$Al apfu) and by B (0.00–0.83 $^{[4]}$B apfu), reflecting a balance between local Al^{3+} and BO_3^{3-} activities during crystallization. The excess negative charge due to the substitution of Al^{3+} and B^{3+} for Si is balanced by $^{[Y]}Al^{3+}$ and $^{[Y]}Fe^{3+}$.
2. Crystallization of the Si-deficient tourmaline was most probably a result of diagenetic processes of evaporate sediments, inducing reactions of quartz and clay minerals as primary components of the sandstone with Ca-saturated, Cl^- and $(BO_3)^{3-}$-rich pore brines. The Cl^- and $(BO_3)^{3-}$ ions could have been delivered to groundwater in desert areas of Upper Rotliegend periodically flooded by water and afterwards drying up, with ephemeral salt lakes, lagoons or a shallow epicontinental sea.

Acknowledgements. We wish to thank two anonymous reviewers and M. Novák for constructive comments that greatly improved the manuscript and the CEMPEG

laboratory at Uppsala University for analyses of the tourmaline with direct determination of B_2O_3 (this is a publication no. 1 of the CEMPEG FE-EPMA laboratory). We also thank V. Janoušek (Editor-in-Chief) for assistance in preparation of the final version of the paper. This work was financially supported by AGH – University of Science and Technology, grant no. 11.11.140.158.

Electronic supplementary material. A table of CAMECA SX 100 electron-microprobe analyses of Si-deficient foitite from the 'Ługi' borehole (B_2O_3 content calculated from stoichiometry) is available online at the Journal web site (*http://dx.doi.org/10.3190/jgeosci.105*).

References

Aljubouri ZA, Aldabbagh SM (1980) Sinjarite, a new mineral from Iraq. Mineral Mag 43: 643–645

Barton R Jr (1969) Refinement of the crystal structure of buergerite and the absolute orientation of tourmalines. Acta Cryst B 25: 1524–1533

Bloodaxe ES, Hughes JM, Dyar MD, Grew ES, Guidotti CV (1999) Linking structure and chemistry in the schorl–dravite series. Amer Miner 84: 922–928

Buniak A (2009) Tourmalines in cement of the Rotliegend sandstone. Przegl Geol 57: 299 (in Polish)

Cempírek J, Novák M, Ertl A, Hughes JM, Rossman GR, Dyar MD (2006) Fe-bearing olenite with tetrahedrally coordinated Al from an abyssal pegmatite at Kutná Hora, Czech Republic: structure, crystal chemistry, optical and XANES spectra. Canad Mineral 44: 23–30

Dunning GE, Cooper JF Jr (1969) A second occurrence of antarcticite, from Bristol Dry Lake, California. Amer Miner 54: 1018–1025

Dyar MD, Francis CA, Wise MA, Guidotti CV, McGuire AV, Robertson JD (1994) Complete chemical characterization of tourmaline. EOS, Trans Amer Geophys Union 75: 187

Dyar MD, Taylor ME, Lutz TM, Francis CA, Guidotti CV, Wise M (1998) Inclusive chemical characterization of tourmaline: Mössbauer study of Fe valence and site occupancy. Amer Miner 83: 848–864

Ertl A, Hughes JM (2002) The crystal structure of an aluminium-rich schorl overgrown by boron-rich olenite from Koralpe, Styria, Austria. Mineral Petrol 75: 69–78

Ertl A, Pertlik F, Bernhardt HJ (1997) Investigation of olenite with excess boron from the Koralpe, Styria, Austria. Öster Akad Wiss Math-Naturw Kl: Anzeiger Abt I 134: 3–10

Ertl A, Hughes JM, Brandstätter F, Dyar MD, Prasad PSR (2003) Disordered Mg-bearing olenite from a granitic pegmatite from Goslarn, Austria: a chemical, structural and infrared spectroscopic study. Canad Mineral 41: 1363–1370

Ertl A, Rossman GR, Hughes JM, Prowatke S, Ludwig T (2005) Mn-bearing "oxy-rossmanite" with tetrahedrally coordinated Al and B from Austria: structure, chemistry, and infrared and optical spectroscopic study. Amer Miner 90: 481–487

Ertl A, Hughes JM, Prowatke S, Ludwig T, Prasad PSR, Brandstätter F, Körner W, Schuster R, Pertlik F, Marschall H (2006) Tetrahedrally coordinated boron in tourmalines from the liddicoatite–elbaite series from Madagascar: structure, chemistry and infrared spectroscopic studies. Amer Miner 91: 1847–1856

Ertl A, Tillmanns E, Ntaflos T, Francis C, Giester G, Körner W, Hughes JM, Lengauer C, Prem M (2008) Tetrahedrally coordinated boron in Al-rich tourmaline and its relationship to the pressure–temperature conditions of formation. Eur J Mineral 20: 881–888

Grice JD, Ercit TS (1993) Ordering of Fe and Mg in tourmaline: the correct formula. Neu Jb Mineral, Mh 165: 245–266

Hancock NJ (1978) Possible causes of Rotliegend sandstone diagenesis in northern West Germany. J Geol Soc, London 135: 35–40

Hawthorne FC (1996) Structural mechanisms for light-element variations in tourmaline. Canad Mineral 34: 123–132

Hawthorne FC, Henry DJ (1999) Classification of the minerals of the tourmaline group. Eur J Mineral 11: 201–215

Henry DJ, Novák M, Hawthorne FC, Ertl A, Dutrow BL, Uher P, Pezzotta F (2011) Nomenclature of the tourmaline-supergroup minerals. Amer Miner 96: 895–913

Hughes JM, Ertl A, Dyar MD, Grew ES, Shearer CK, Yates MG, Guidotti CV (2000) Tetrahedrally coordinated boron in a tourmaline: boron-rich olenite from Stoffhütte, Koralpe, Austria. Canad Mineral 38: 861–868

Hughes KA, Hughes JM, Dyar MD (2001) Chemical and structural evidence for $^{[4]}B \leftrightarrow {}^{[4]}Si$ substitution in natural tourmalines. Eur J Mineral 13: 743–747

Hughes JM, Ertl A, Dyar MD, Grew ES, Wieden-Beck M, Brandstätter F (2004) Structural and chemical response to varying $^{[4]}B$ content in zoned Fe-bearing olenite from Koralpe, Austria. Amer Miner 89: 447–454

Jackowicz E (1994) Permian volcanic rocks of the northern part of the Sudetic monocline. Prace Państw Inst Geol 145: 47 (in Polish)

Kalt A, Schreyer W, Ludwig T, Prowatke S, Bernhardt HJ, Ertl A (2001) Complete solid solution between magnesian schorl and lithian excess-boron olenite in a pegmatite from Koralpe (eastern Alps, Austria). Eur J Mineral 13: 1191–1205

Karnkowski PH (1987) Lithostratygraphy of Rotliegend in Wielkopolska. Geol Quart 31: 643–672 (in Polish)

Kiersnowski H (1997) Depositional development of the Polish Upper Rotliegend Basin and evolution of its sediment source areas. Geol Quart 41: 433–456

Lussier AJ, Aguiar PM, Michaelis VK, Kroeker S, Hawthorne FC (2009) The occurrence of tetrahedrally coordinated Al and B in tourmaline: an ^{11}B and ^{27}Al MAS NMR study. Amer Miner 94: 785–792

MacDonald DJ, Hawthorne FC (1995) The crystal chemistry of Si↔Al substitution in tourmaline. Canad Mineral 33: 849–858

Marler B, Ertl A (2002) Infrared and NMR spectroscopic study of excess-boron olenite from Koralpe, Styria, Austria. Amer Miner 87: 364–367

Marler B, Borowski M, Wodara U, Schreyer W (2002) Synthetic tourmaline (olenite) with excess boron replacing silicon in the tetrahedral site: II. Structure analysis. Eur J Mineral 14: 763–771

Marschall HR, Ertl A, Hughes JM, McCammon C (2004) Metamorphic Na- and OH-rich disordered dravite with tetrahedral boron, associated with omphacite, from Syros, Greece: chemistry and structure. Eur J Mineral 16: 817–823

Pokorski J (1981) A proposition of formal lithostratigraphic division of Rotliegend in the Polish Depression. Geol Quart 25: 41–58 (in Polish)

Pokorski J (1988) Evolution of the Rotliegendes Basin in Poland. Bull Pol Acad Sci, Earth Sci 37: 49–55

Pouchou JL, Pichoir F (1985) "PAP" (φρZ) procedure for improved quantitative microanalysis. In: Armstrong JT (ed) Microbeam Analysis. San Francisco Press, San Francisco, pp 104–106

Povondra P (1981) The crystal chemistry of tourmalines of the schorl–dravite series. Acta Univ Carol, Geol 3: 223–264

Prowatke S, Ertl A, Hughes JM (2003) Tetrahedrally coordinated Al in Mn-rich, Li- and Fe-bearing olenite from Eibenstein an der Thaya, Lower Austria: a chemical and structural investigation. Neu Jb Mineral, Mh 2003: 385–395

Schreyer W, Wodara U, Marler B, van Aken PA, Seifert F, Robert JL (2000) Synthetic tourmaline (olenite) with excess boron replacing silicon in the tetrahedral site: I. Synthesis conditions, chemical and spectroscopic evidence. Eur J Mineral 12: 529–541

Schreyer W, Hughes JM, Bernhardt HJ, Kalt A, Prowatke S, Ertl A (2002) Reexamination of olenite from the type locality: detection of boron in tetrahedral coordination. Eur J Mineral 14: 935–942

Serdyuchenko DP (1980) Different position of boron in tourmaline lattices. Dokl AN USSR 254: 177–179 (in Russian)

Tagg SL, Cho H, Dyar MD, Grew ES (1999) Tetrahedral boron in naturally occurring tourmaline. Amer Miner 84: 1451–1455

Wodara U, Schreyer W (1997) Turmaline mit Borüberschuß im System Na_2O–Al_2O_3–B_2O_3–SiO_2–H_2O (NABSH). Berichte der Deutschen Mineralogischen Gesellschaft, Beihefte z Eur J Mineral 9: 394

Wodara U, Schreyer W (1998) Tetrahedral boron in tourmalines of the system Na_2O–Al_2O_3–B_2O_3–SiO_2–H_2O. Terra Nova 10 (abstracts supplement no. 1): 68–69

Wodara U, Schreyer W (2001) X-site vacant Al-tourmaline: a new synthetic end-member. Eur J Mineral 13: 521–532